ROS-Induced Oxidative Stress Causes Enrichment and Emergence of Antibacterial Resistance in Conventional Activated Sludge Process

*Bharat Manna[1], Xueyang Zhou[1], and Naresh Singhal[1,2] **

[1]Department of Civil and Environmental Engineering, University of Auckland, Auckland 1142, New Zealand

[2]Water Research Centre, University of Auckland, Auckland 1142, New Zealand

*Corresponding author: n.singhal@auckland.ac.nz

ABSTRACT

Conventional activated sludge (CAS) processes represent significant reservoirs of antibacterial resistance genes (ARGs). However, the mechanisms governing ARG proliferation (enrichment and emergence) in CAS remain poorly understood. We hypothesize that Reactive Oxygen Species (ROS), generated by oxygenation in aeration tanks, govern ARG proliferation. Shotgun-metagenomics assessment of ARG abundance across treatment stages of two plants handling hospital effluents revealed a substantial reduction in total ARGs in treated effluent. However, specific ARGs conferring resistance to beta-lactams, tetracyclines, aminoglycosides, rifamycins, macrolides, and other drug classes showed marked increase in CAS, exhibiting correlations with ROS stress response genes. Notably, many of these ARGs emerged in the CAS and were absent in upstream processes. Proof-of-concept experiments demonstrated increased ROS and ARG levels under high dissolved oxygen (8 mg/L) compared to low oxygen (2 mg/L) conditions. Both ESKAPE and non-ESKAPE host pathogens in CAS harbored multiple shared ARGs, indicating horizontal gene transfer facilitated proliferation. ROS-induced stress responses, including antioxidant defense activation, cell damage, DNA mutation, metabolic adaptation, efflux pump activation, and enhanced transformation, could contribute to ARG enrichment/emergence. This study highlights that oxygenation in CAS inadvertently promotes ARG proliferation, underscoring the need to manage oxygen levels to control ROS-induced ARG proliferation and environmental dissemination.

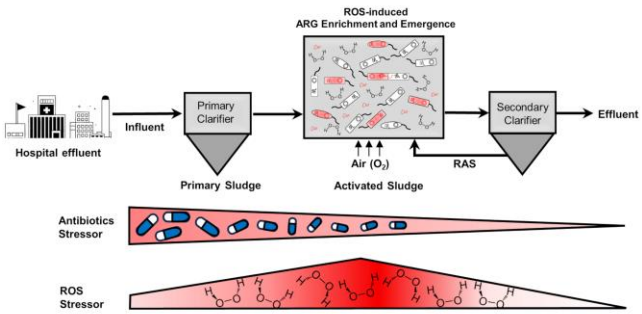

KEYWORDS: activated sludge, oxygenation, antibiotic resistance, reactive oxygen species, horizontal gene transfer, stress response, metagenomics

INTRODUCTION

Antibiotic resistance (AR) poses an escalating threat to global public health, responsible for approximately 1.27 million fatalities worldwide and contributing to almost an estimated 4·95 million (3·62–6·57) deaths associated with bacterial antimicrobial resistance in 2019 [1]. In the United States alone, infections afflict over 2.8 million individuals annually, leading to the deaths of more than 35,000 people [2]. The financial burden of managing infections caused by six prevalent antibiotic-resistant bacteria (ARB)[1] (*Escherichia coli*, *Staphylococcus aureus*, *Klebsiella pneumoniae*, *Streptococcus pneumoniae*, *Acinetobacter baumannii*, and *Pseudomonas aeruginosa*), especially within healthcare settings exceeds $4.6 billion each year [3]. Antibiotic resistance is a critical One Health issue [4], profoundly affecting humans, animals, and the environment, impacting even the most fundamental resource for life: water. The presence of antibiotic-resistant genes (ARGs) and ARBs often can be attributed to effluents from hospitals, farms, and sewage systems, illustrating the interconnectedness of human activities and the broader environmental impact of AR [5–8]. As wastewater treatment plants (WWTPs) operate at the human-environment interface, they play a crucial role in both managing and understanding the global health effects of AR [9–11]. WWTPs receive and process diverse influents, including hospital effluents laden with high concentrations of antibiotics, ARBs, and ARGs [12–14]. This influx creates a potent selection pressure for ARGs and facilitates horizontal gene transfer (HGT) among bacterial communities [14–16]. Notably, hospital wastewaters harbor ARG concentrations several orders of magnitude higher than municipal wastewater [17], highlighting their alarming potential to seed and propagate resistance within WWTPs treating such influents [18–20]. Moreover, recent studies reported that different WWTP treatment processes could exhibit varying impacts on ARG and ARB dynamics [21–23]. Interestingly, the authors identified

55 significant alteration in the ARGs composition in the sludge compared to the of the influent
56 resistome and suggested seasonality in antimicrobial use to be key influencing factor behind this
57 transition [21]. Another study combining multi-omics approach also revealed that both absolute
58 and relative ARG transcript abundance of the conventional activated sludge (CAS) resistome
59 were significantly enriched with specific ARGs drug classes (multidrug, beta-lactam,
60 aminoglycoside, tetracycline, vancomycin etc.) compared to the influent ARG composition,
61 suggesting bacterial community composition and biomass concentration to be key factors [24].
62 Many other reports also identified CAS processes as a potential hotspots for ARG enrichment
63 [23,25–27]. These enriched ARGs in CAS contribute significantly to the effluent resistome which is
64 disseminated into the receiving environment [21,23,24]. However, the specific mechanisms driving
65 the enrichment and emergence of ARGs within CAS processes remain poorly understood.
66 Consequently, understanding the underlying mechanisms behind the emergence of ARGs in CAS
67 processes has become an urgent need.
68 While antibiotics are relatively recent human inventions, microbes have developed resistance
69 mechanisms over thousands of years through their continuous evolutionary struggle for survival
70 [28]. Recent evidence suggests a unifying mechanism behind the action of many bactericidal
71 antibiotics, where reactive oxygen species (ROS) generation plays a key role behind lethality [29–
72 31]. ROS like hydrogen peroxide (H_2O_2), hydroxyl radical ($OH^{\cdot}$), singlet oxygen ($^1O_2$), and
73 superoxide anion (O_2^-) are inherent byproducts of bacterial aerobic respiration [32,33]. Furthermore,
74 ROS-mediated killing can trigger a secondary stress response beyond the initial antibiotic-
75 induced damage, involving factors like activation of response regulators (*e.g.*, *ArcA*), metabolic
76 reprogramming of the TCA cycle, and disruption of the nucleotide pool with increased ATP
77 demand [34]. Notably, ROS-mediated killing is also a weapon in the arsenal of various innate host

78 defense systems [35]. To counter this oxidative stress and survive, bacteria have evolved diverse
79 antioxidant defenses through metabolic remodeling. These include overproduction of ROS-
80 scavengers, activation of alternative metabolic pathways like the glyoxylate shunt (GS) and
81 pentose phosphate pathway (PPP), and enhanced substrate-level phosphorylation [34]. However,
82 bacterial efforts to develop ROS tolerance often come at a cost. The increased oxidative stress
83 can lead to direct DNA damage, potentially triggering novel mutations, and ultimately
84 contributing to the emergence of AR [36–39]. Since ROS are common to both antibiotic action and
85 bacterial stress responses, resistance to ROS could be a key shared characteristic underlying
86 ARG development.
87 The significance of ROS in CAS processes can be attributed to the constant aeration inherent to
88 these systems, which creates a unique environment characterized by high dissolved oxygen (DO)
89 levels and, consequently, elevated ROS generation. While existing research hints at the
90 connection between ROS and ARG emergence in the context of WWTP, it primarily focuses on
91 lab experiments and specific antibiotics or stressors. One study observed a significant increase in
92 antibiotic resistance in *Escherichia coli* exposed to aeration tanks compared to primary or final
93 sedimentation tanks [40]. Another study linked triclosan-induced oxidative stress to a rise in ARGs,
94 particularly tetracycline and multidrug resistance genes [41]. Similarly, ROS generated by phenolic
95 compounds have been proven to promote resistance through increased membrane permeability
96 and HGT [42]. Moreover, antidepressant fluoxetine induced resistance to multiple antibiotics (*e.g.*,
97 fluoroquinolone, aminoglycoside, β-lactams, tetracycline and chloramphenicol) in *Escherichia*
98 *coli* via ROS-mediated mutagenesis [39]. Despite these findings, the critical question of whether
99 aeration-induced ROS in real-world WWTPs shape the multifaceted resistome in CAS processes,
100 remains unanswered.

101 We hypothesize that oxidative stress resulting from high DO levels plays a pivotal role in
102 fostering the development of antibiotic resistance within the CAS processes. We propose to
103 assess the hypothesis by investigating how aeration influences ROS generation leading to ARGs
104 induction and impact on the ARGs within CAS compared to hospital effluents and WWTP
105 influent. In recent years, metagenomic approaches have revolutionized WWTP surveillance,
106 enabling comprehensive profiling of resistomes [8,24,43,44]. By analyzing shotgun metagenomic data
107 from two full-scale WWTPs treating hospital effluents, we assess whether aeration in CAS
108 processes influences alteration in ARG abundance and, crucially, whether ROS stressors
109 correlate with the specific enriched and emerged ARGs.

110 **MATERIALS AND METHODS**

111 **Sample data collection**

112 In this work, we considered paired-end shotgun metagenomics samples obtained using a HiSeq
113 2500 instrument from two full-scale WWTPs processing university hospital effluents in
114 Göttingen ($WWTP_{Gö}$), and Greifswald ($WWTP_{Gw}$), Germany [45]. The samples were collected
115 from five different stages (abbreviated as S) from both the WWTPs, *i.e.*, S1: Hospital effluent (a
116 storage tank next to the university hospital), S2: WWTP Influent, S3: Primary Sludge, S4:
117 conventional activated sludge (CAS), and S5: WWTP effluent as described elsewhere [45,46]. The
118 details of the sample names, and NCBI SRA accession used in this study, can be found in the
119 Table S1 and Table S2. The raw metagenomes can be accessed in the NCBI Sequence Read
120 Archive under the BioProject accession number PRJNA524094 [46].

121 **Metagenomics Analysis**

122 We performed preprocessing steps to eliminate low-quality sequences using Trimmomatic [47]
123 with specific quality thresholds: LEADING:3, TRAILING:3, SLIDINGWINDOW:10:15, and

MINLEN:50 with the following settings: TruSeq3-PE-2.fa:2:30:10:2:keepBothReads [48]. For metagenomic taxonomic and functional profiling, we employed the SqueezeMeta v1.5.2 pipeline [49]. The read statistics per sample is provided in Table S1 and Table S2. Co-assembly was performed using Megahit [50], and short contigs (<200 bps) were filtered out using prinseq [51]. Within the SqueezeMeta pipeline, Barrnap [52] tool was used for predicting RNAs, while Prodigal [53] was utilized for predicting ORFs. Similarity searches against NCBI GenBank nr database [54] and Kyoto Encyclopedia of Genes and Genomes [55], were performed for taxonomic and functional assignments, respectively, using Diamond [56] with a maximum e-value threshold of 1e-03. Moreover, the Comprehensive Antibiotic Resistance Database [57] release 3.2.4 was used for annotating the ARGs and identifying the ARBs in metagenomics data. Bowtie2 [58] was used for read mapping against the contigs. The metagenomics data was analyzed using the SQMtools R package [59].

Bioinformatics Analysis and Visualization

We used Cumulative Sum Scaling [60] (CSS) to normalize both taxa and gene raw read sequence counts. To assess the diversity of ARG composition across the different treatment stages, we calculated a Bray-Curtis dissimilarity matrix with PERMANOVA to determine the significance of clustering, using MicrobiomeAnalyst [61]. A heatmap was plotted to visualize changes in the abundance of each ARG, utilizing a z-score with TBtools [62]. Furthermore, differentially enriched/emerged ARGs in CAS (S4) were identified using EdgeR [63] with an adjusted p-value cutoff of 0.05. The correlation between ROS stressor genes and differentially abundant ARGs was performed using a Mantel test (p-value < 0.05), while the co-association network between the ARGs and ARB pathogens was constructed using the Sparse Correlations for Compositional data (SparCC) [64] correlation ($r > 0.6$ and p-value < 0.05) method. Both correlation analyses were

147 conducted using OmicStudio tools (https://www.omicstudio.cn/). The co-association network
148 was visualized with Gephi [65] version 1.10.1. Graphics were generated using the ggplot2 [66]
149 package in R [67] version 4.2.1.

150 **Batch reactor experiments with different DO levels**

151 In order to validate our hypothesis of higher ROS generation under more oxidative stress leading
152 to increased ARGs, we performed batch reactor experiments with CAS samples under low (2
153 mg/L) and high (8 mg/L) DO levels. The CAS samples were obtained from the Māngere WWTP
154 in Auckland, New Zealand. The experiments were conducted in reactors with a capacity of 1 L,
155 at a temperature of 20 °C. Each liter of the microbial reaction solution contained 2.75 g/L of
156 mixed liquor suspended solids (MLSS) activated sludge, 3.84 g/L of sodium bicarbonate as the
157 inorganic carbon source, and 1 mL of trace element solution (Table S3). Over the course of the
158 48-hour experiment, a total of 50 mL of concentrated artificial wastewater (Table S4) was
159 uniformly and continuously added into the system using a syringe pump and mixed using a
160 magnetic stirrer. Detailed methodology for ROS measurement and DNA extraction for
161 metagenomics analysis are provided in the Supporting Information. The raw metagenome
162 samples from these experiments can be accessed in the European Nucleotide Archive under the
163 BioProject accession number PRJEB74089 as provided in Table S5.

164 **RESULTS AND DISCUSSION**

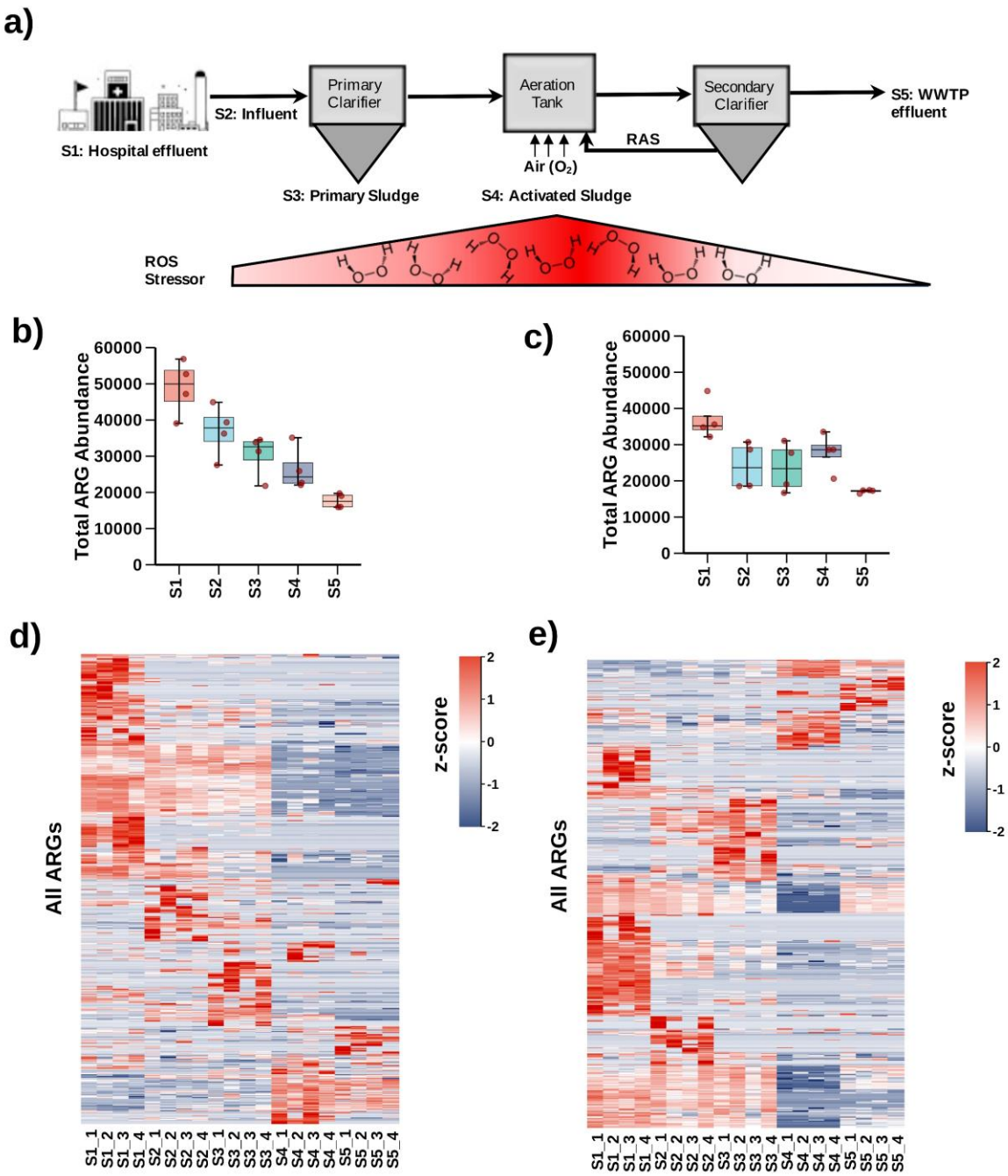

Figure 1. Alteration of ARG abundance across different WWTP stages. (a) Schematic representation of the WWTP stages studied, including S1: Hospital effluent, S2: WWTP influent, S3: Primary sludge, S4: Activated sludge, and S5: WWTP effluent. The variation in ROS stressor levels across these stages is depicted below. (b) and (c) show the total relative ARG abundance at each stage for $WWTP_{Gö}$ and $WWTP_{Gw}$, respectively. Heatmaps display the trend of change in each ARG relative abundance across the stages in (d) $WWTP_{Gö}$ and (e) $WWTP_{Gw}$ with a prominent set of enriched (or emerged) ARGs (red) in both S4 and S5. RAS: Recycled activated sludge.

172 **Comparison of ARG abundances across different treatment stages**

173 In this study, we systematically analyzed and compared metagenomic samples from various
174 stages of wastewater treatment processes to assess changes in the resistome profile. These stages
175 included hospital effluents (S1), WWTP influent (S2), primary treatment (S3), CAS (S4), and
176 WWTP effluents (S5) (Figure 1a). Our findings showed a significant decrease in total ARG
177 abundances at different stages of $WWTP_{Gö}$ compared to the hospital effluents: 24.38% in S2,
178 37.95% in S3, 46.04% in S4, and 63.89% in S5 (Figure 1b). Moreover, the number of ARGs also
179 exhibited reductions: 28.27% in S2, 29.39% in S3, 51.92% in S4, and 63.74% in S5 (Figure
180 S1a). A similar analysis conducted in the $WWTP_{Gw}$ also revealed a reduction in ARG
181 abundances of 34.48% in S2, 35.86% in S3, 24.45% in S4, and 53.50% in S5, compared to S1
182 (Figure 1b). The numbers of ARGs detected at these stages also decreased by 25.24% in S2,
183 30.95% in S3, 67.78% in S4, and 45.40% in S5 (Figure S1c). The highest abundance of ARGs
184 was observed in the hospital effluent (S1) for both WWTPs, which is expected due to the
185 prevalent use of antibiotics in hospital settings, leading to a higher presence of ARGs. Across the
186 treatment stages, a consistent trend of ARG reduction was noted, indicating the effectiveness of
187 the WWTP processes in decreasing the overall ARG abundance in the effluent (S5). This pattern
188 of ARG reduction in CAS and effluents are in agreement with previous metagenomics-based
189 studies [21,26,44].

190 Furthermore, the diversity of resistome profiles across various stages of the $WWTP_{Gö}$ and
191 $WWTP_{Gw}$ was evaluated using principal coordinate analysis (PCoA) with a Bray-Curtis
192 dissimilarity matrix (Figure S1b, d). The PCoA demonstrated clear clustering of resistomes
193 corresponding to the five treatment stages. In $WWTP_{Gö}$, the analysis accounted for 79.33% of the
194 variation (R^2: 0.79329), with significant separation observed (PERMANOVA F-value: 14.392,

195 p-value: 0.001), indicating distinct ARG profiles at each treatment stage. Similarly, $WWTP_{Gw}$'s
196 resistome profiles were markedly segregated, explaining a higher variance of 83.56% (R^2:
197 0.83563) and demonstrating substantial differentiation (PERMANOVA F-value: 19.064, p-
198 value: 0.001). The PCoA results showed that the resistomes from hospital effluent (S1), WWTP
199 influent (S2), and primary treatment (S3) stages clustered closely, suggesting similar ARG
200 compositions, possibly due to the direct contribution of hospital effluent to the influent. In
201 contrast, samples from the CAS (S4) and treated effluent (S5) stages were distinctly separate
202 from the preceding stages. This delineation reflects a significant transition in the ARG profile,
203 attributable to the biological processes and selection pressure within the activated sludge system
204 and secondary clarifiers. The distinct clusters for the S4 and S5 stages also suggest that the both
205 the CAS, and effluent harbors unique ARG composition, with potential environmental
206 implications upon its release. Similar variation in resistome in influent, activated sludge and
207 effluent have been reported in previous studies [21,23].
208 In addition to the overall trend analysis, a detailed heatmap of all ARGs based on normalized
209 abundance z-scores was generated to further elucidate the specific changes in ARG profiles at
210 each treatment stage, with a focus on the CAS (S4) process (Figure 1d, e). The heatmap
211 illustrated that while some ARGs were consistently abundant across all stages, others were more
212 stage specific. This abundance pattern reinforces the notion of stage-specific selective pressures
213 and microbial community dynamics shaping the ARG profile. Interestingly, despite the general
214 trend of decreasing total ARG abundance (Figure 1b, c), certain ARGs exhibited notable
215 persistence and remarkable enrichment/emergence in the CAS stage (S4) in both the WWTPs
216 (Figure 1d, e). This relative enrichment of ARGs in the CAS was previously reported using
217 combined metagenomics and metatranscriptomics study [24].

218 **Identifying the enriched and emerged ARGs in CAS process**

219 To enhance our understanding of the enriched or emerged ARGs within the CAS process, we
220 conducted a detailed analysis of ARGs that were differentially higher abundant in CAS than the
221 upstream stages. Specifically, in the $WWTP_{Gw}$ facility, we observed that 111, 115, and 116
222 ARGs exhibited significantly (FDR < 0.05) higher abundance in CAS when compared to
223 hospital effluent (S1), influent (S2), and primary treatment stages (S3), respectively, as
224 illustrated in Figure 2a. Similarly, for the $WWTP_{Gö}$ facility, 152, 138, and 114 ARGs were found
225 to be more abundant in CAS relative to the same comparator stages (hospital effluent, influent,
226 and primary treatment) (Figure S2a). Additionally, certain ARGs were identified as being
227 significantly more abundant in S4 compared to all other stages (S1, S2, and S3), with some
228 ARGs being uniquely abundant to specific treatment stages (Figure S3 and Supplemental Data
229 1). To facilitate downstream analyses, we compiled a list of ARGs that were significantly
230 abundant in the CAS process, selecting those genes that displayed a higher average abundance in
231 CAS compared to all preceding treatment stages. This analysis yielded a total of 139 and 106
232 highly abundant ARGs for $WWTP_{Gö}$ and $WWTP_{Gw}$, respectively, as detailed in Supplemental
233 Data 2a. Notably, 17.27% ($WWTP_{Gö}$) and 19.81% ($WWTP_{Gw}$) of the ARGs were not detected at
234 any of the upstream stages, suggesting they emerged under the selection pressure of the CAS
235 process (Supplemental Data 2b). These emerged ARGs exhibited resistance to aminoglycoside
236 (*AAC(3)-IIIc*, *AAC(6')-Iih*), beta-lactam (*OXA-34*, *OXA-660*, *OXA-4*, *GOB-3*, *GOB-4*, *IDC-2*,
237 *IMP-1*, *IMP-13*, *IMP-28*), rifamycin (*iri*, *arr-1*), tetracycline (*tap*, *tet(V)*), glycopeptide (*vanD*,
238 *vanI*), and other antibiotics. Additionally, among the enriched ARGs in both WWTPs were those
239 belonging to various beta-lactamases, such as *OXA* (including *OXA-2*, *OXA-45*, *OXA-101*, *OXA-*
240 *129*, *OXA-198*) beta-lactamases. These ARGs confer resistance to antibiotics like carbapenems,

241 cephalosporins, and penams, highlighting a significant selection pressure for beta-lactam
242 resistance. This is especially concerning given the extensive use of beta-lactam antibiotics and
243 the potential for these resistance mechanisms to spread into the environment. Furthermore, we
244 identified multiple ARGs conferring resistance to other antibiotic classes, including tetracycline
245 (*tet(35)*, *tet(49)*, *tet(G)*, *tet(O/32/O)*, *tet(T)* etc.), glycopeptide (*vanC*, *vanF*, *vanS_in_vanC_cl*,
246 etc.), and aminoglycoside (*AAC(3)-Id*, *AAC(6')-32*, *AAC(6')-Ic*, *AAC(6')-IIa*, *AAC(6')-IIb*,
247 *AAC(6')-IIc*, *aadA*, *amrB*, etc.), among others. Resistance to rifamycin (*rpoB2*, *Bado_rpoB_RIF*,
248 *Nfar_rox*, *rphA*, *rphB,*), macrolide (*EreA2*, *EreB*, *mphA*), fluoroquinolone (*QepA4*, *QnrS6*,
249 *QnrS8*), and sulfonamide (*sul2*, *sul4*) antibiotics were also observed, alongside ARGs resistant to
250 multiple antibiotics, such as *AxyY*, *efrB*, *MexF*, *mexP*, *mexQ*, *mexY*, *opmE*, *smeE*, and more, as
251 provided in Supplemental Data 2a. Consistent with our observations, a significant enrichment of
252 various resistance genes, including those encoding for beta-lactamases, macrolides, and
253 tetracyclines, was identified in recirculated activated sludge in comparison to primary sludge [26].
254 This enrichment was suggested due to the selective pressure within the wastewater treatment
255 facility. Similarly, previous research documented an escalation in the relative abundance of a
256 wide array of ARGs, spanning multiple drug classes such as beta-lactamases, aminocoumarins,
257 glycopeptides, rifamycins, and sulfonamides, from influent to effluent in a conventional WWTP
258 [23]. Furthermore, another study reported an increase in both the transcript and gene abundance of
259 various ARG classes, including Multidrug, beta-lactamases, aminoglycosides, tetracyclines,
260 trimethoprim, and vancomycin, in secondary effluent compared to the influent of post-primary
261 clarifiers [24]. Additionally, it was found that aerobic biomass exhibited a higher overall abundance
262 of ARGs compared to anaerobic and anoxic biomass, with a notable increase in effluent
263 abundances of fluoroquinolone and tetracycline ARGs [27]. These observations underscore the

diverse spectrum of resistant ARGs emerging within the CAS process, indicating that while the CAS process effectively reduces the overall ARG load, it also inadvertently facilitates the proliferation (enrichment and emergence) of multiple concerning ARGs.

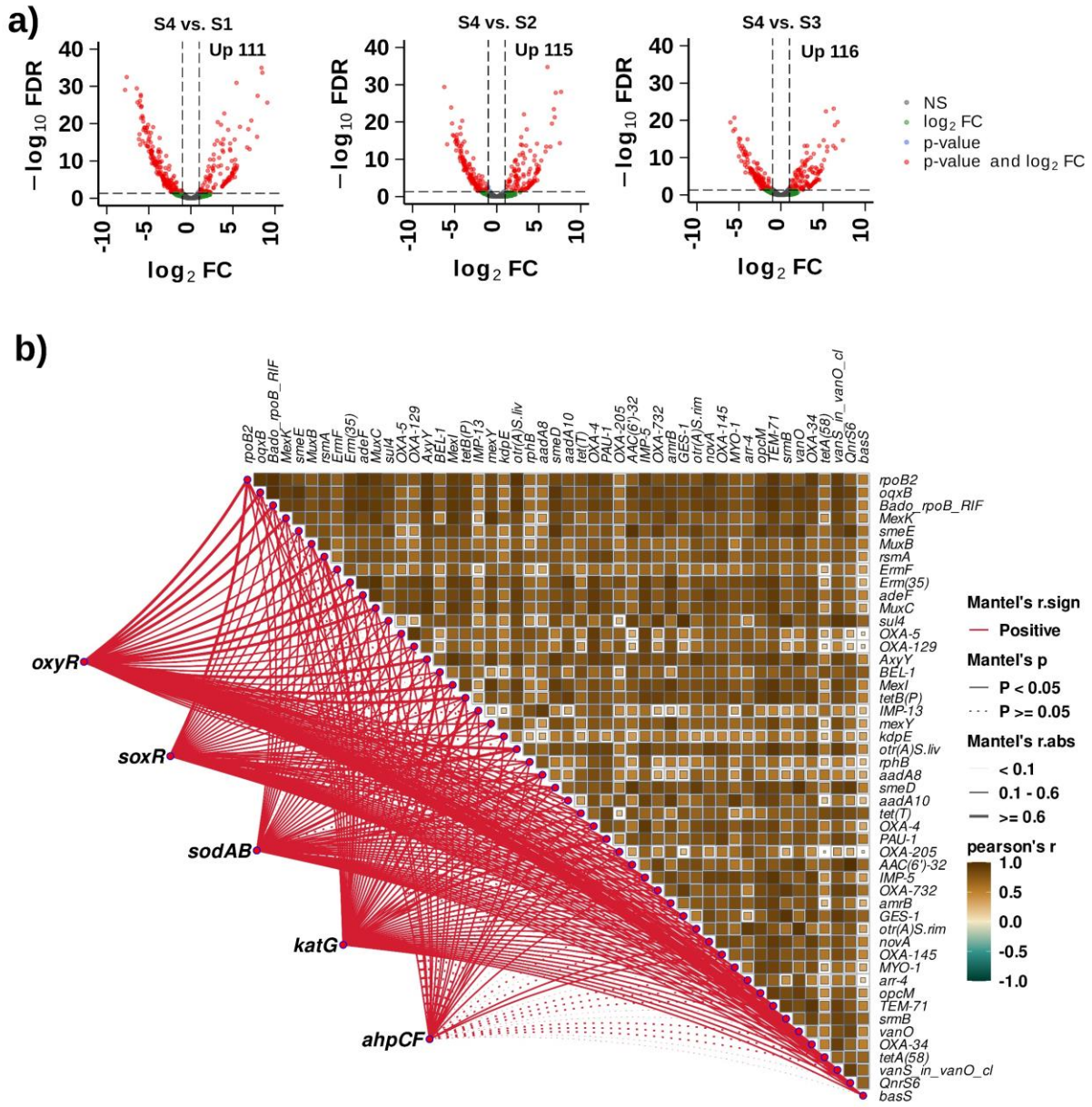

Figure 2. Differentially enriched (or emerged) ARGs and their correlation network with ROS stressors in the CAS process. a) Volcano plots illustrating the differentially abundant ARGs in the CAS stage compared to S1: Hospital effluent, S2: WWTP influent, S3: Primary sludge in the $WWTP_{Gw}$. The grey and red colors indicate the

nonsignificant and significant ARGs, respectively. b) A network analysis depicting the correlations between selected enriched/emerged ARGs and ROS stress response genes in CAS process in $WWTP_{Gw}$.

Assessing the correlation between the ROS stressors and enriched or emerged ARGs

We hypothesized that ROS generated from aeration in the CAS contributes to ARG enrichment/emergence in the CAS process. To explore this, we examined the relationship between key genes involved in ROS stress response and the enriched/emerged ARGs found in CAS of both the WWTPs. We focused on five crucial ROS-related genes [68]: two transcription factors, *oxyR* and *soxR*, which play key roles in the cellular response to oxidative stress, and three genes encoding enzymes that help detoxify ROS, namely *sodAB* (Superoxide dismutase), *katG* (Catalase-peroxidase), and *ahpCF* (alkyl hydroperoxide reductase). Notably, previous reports revealed *oxyR* [69,70] and *soxRS* [71] contributed to virulence in *E. coli*, *Pseudomonas aeruginosa*, and *Salmonella enterica*. Our analysis revealed a significant correlation between these ROS stress response genes and numerous ARGs in both WWTPs (Figure 2b, Figure S2b, Supplemental Data 3). Specifically, in the $WWTP_{Gö}$, the number of ARGs positively correlated with each ROS stressor were as follows: *oxyR* (24), *soxR* (42), *sodAB* (65), *katG* (65), and *ahpCF* (35). Meanwhile, in $WWTP_{Gw}$, the numbers of ARGs linked to the same stressors were *oxyR* (81), *soxR* (71), *sodAB* (63), *katG* (92), and *ahpCF* (25). These findings indicate that the mechanisms bacteria use to cope with oxidative stress, including the activation of specific genes and detoxification enzymes, may play a role in the proliferation of ARGs in CAS environment. In the case of $WWTP_{Gö}$, a total of 14 ARGs were identified as having correlations with all ROS stressors (Figure S4a). These ARGs encompass a diverse array of resistance mechanisms, including multidrug resistance (*e.g.*, *mexY*), beta-lactamases (*OXA-4*, *PAU-1*, *AQU-3*) which provide resistance to beta-lactam antibiotics, tetracycline resistance (*tet(T)*), macrolide resistance (*mtrA*), and various others (*lmrC*, *rpoB2*, *Bado_rpoB_RIF*, *rphB*, *dfrB6*, *sul4*, *adeF*, *arr-1*,

295 *vanR_in_vanE_cl*). Furthermore, a significant cohort of 23 ARGs, including *OXA* variants (*OXA-*
296 *9*, *OXA-21*, *OXA-129*, *OXA-37*), metallo-beta-lactamases (*IMP-13*, *IMP-28*), and others (*MYO-1*,
297 *GOB-4*, *vanS* in various clusters, *vanD*, *aadA8*, *AxyY*, *efrB*, *Cstr_tetA*, *rsmA*, *AAC(6')-IIa*, *dfrB2*,
298 *AAC(6')-Iih*, *PEDO-1*, *BRP(MBL)*, *opcM*), showed correlation with the antioxidant enzymes
299 *sodAB* and *katG*, indicating a broad spectrum of antibiotic resistance mechanisms being
300 influenced by oxidative stress responses. Besides, within the $WWTP_{Gw}$, 17 ARGs were
301 correlated with all ROS stressors, including genes responsible for multidrug resistance (*MuxB*,
302 *MuxC*, *AxyY*), beta-lactamase activity (*OXA-4*, *OXA-5*, *OXA-145*, *IMP-5*, *PAU-1*), tetracycline
303 resistance (*tet(T)*, *tetB(P)*), and rifamycin resistance (*rphB*, *rpoB2*), among others (*rsmA*, *adeF*,
304 *BEL-1*, *aadA8*, *novA*) (Figure S4b). Additionally, a noteworthy observation was the correlation
305 of a considerable number of ARGs with multiple ROS stressors, specifically 27 ARGs
306 correlating with *soxR*, *oxyR*, *sodAB*, and *katG*, and 20 ARGs correlating with *soxR*, *oxyR*, and
307 *katG*. This pattern underscores the intricate relationship between oxidative stress response
308 mechanisms and the proliferation of antibiotic resistance within these CAS processes. Previous
309 research reported that *Escherichia coli K12* resistant to multiple antibiotics (chloramphenicol,
310 amoxicillin and tetracycline) produced significantly higher levels of ROS compared to the wild-
311 type [39]. Additionally, the resistant strains also exhibited significant overexpression of ROS
312 scavengers including *sodA* and *ahpF*. A recent study showed that exposure to bactericidal
313 antibiotics (amoxicillin, enrofloxacin, and kanamycin) increased ROS production in the *oxyR*
314 knocked out *E. coli* compared to the wild-type [36]. Moreover, heme induced electron transport
315 chain enhanced the ROS production leading to *de novo* acquired resistance in *Lactobacillus*
316 *lactis* [36]. These reports support our findings on the pattern of correlations and underscore the
317 potential link between ROS stressors and ARG emergence. A notable aspect of our findings is

the identification of common and unique ARGs across different ROS stressors. Certain ARGs appear frequently across multiple ROS stressor correlations, suggesting that these ARGs might be more universally responsive to ROS-induced stress. In contrast, unique ARGs correlating with specific ROS stressors indicate targeted responses to particular oxidative stress conditions. This analysis hinges on our hypothesis that the ROS generated during the aeration process in CAS are instrumental in inducing the enrichment of ARGs. Through a meticulous examination of various ROS stressor genes and their correlations with the differentially enriched ARGs, we have uncovered patterns that reinforce this hypothesis and provide insights into the mechanisms driving the ARG enrichment/emergence.

Experimental support for increased ARG abundance and ROS under high DO

To further elucidate the potential influence of ROS on the enrichment/emergence of ARGs within the CAS process, we conducted a series of batch reactor experiments employing CAS samples derived from the Māngere WWTP in Auckland, New Zealand. This approach was tailored to mimic the oxidative conditions prevalent in the CAS process, focusing particularly on the variation of DO concentrations.

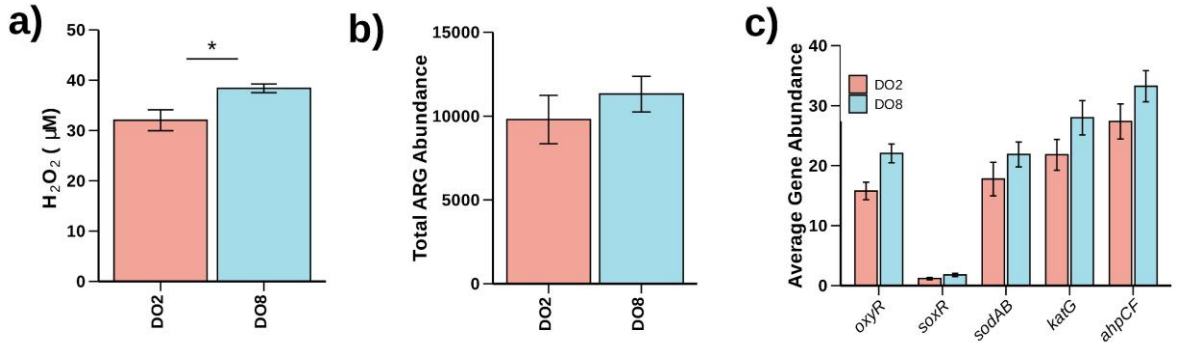

Figure 3. Impact of DO levels on ROS production and ARG abundance. a) Bar graph representing the concentration of H_2O_2 under DO2 and DO8, indicating a statistically significant increase in ROS at higher DO levels (* $p < 0.05$). b) Comparative total relative ARG abundance showing a moderate increase at elevated DO levels (DO8) in

337 comparison to lower DO levels (DO2). c) The bar graph illustrates the average relative abundance of oxidative stress
338 response genes in DO2 and DO8 conditions, reflecting an upregulation in response to increased DO concentration.

339 Specifically, our experimental design encompassed two distinct DO concentrations, namely,
340 DO2 (2 mg/L) and DO8 (8 mg/L), to evaluate the impact of elevated DO levels on ROS
341 generation. Quantitative analysis of hydrogen peroxide (H_2O_2) concentrations yielded average
342 concentrations of 32.05 ± 2.08 μM and 38.38 ± 0.86 μM for DO2 and DO8 conditions,
343 respectively (Figure 3a). These results suggest a slight elevation in ROS levels in response to an
344 increase in DO concentration. Subsequent analysis focused on the total abundance of ARGs
345 across varying DO levels further underscored similar trends. Specifically, the relative abundance
346 of total ARGs exhibited a moderate increment under the DO8 condition (11312.57±1065.84)
347 when compared to the lower DO2 level (9799.61±1442.85) (Figure 3b). Interestingly, a similar
348 resistome profile observed in CAS of both $WWTP_{Gö}$ and $WWTP_{Gw}$ was detected in the DO
349 experiments. Among these, prevalent ARG classes included aminocoumarin antibiotics,
350 aminoglycosides, beta-lactams (encompassing carbapenems, cephalosporins, penams),
351 fluoroquinolones, macrolides, tetracyclines, peptide antibiotics, rifamycins, and sulfonamides
352 (Figure S5a). These ARG resistant drug classes were also observed in both the CAS processes in
353 the $WWTP_{Gö}$, and $WWTP_{Gw}$ (Figure S5 b, c). Notably, a significant proportion of these ARGs
354 demonstrated enrichment under the DO8 condition in comparison to DO2, with multiple
355 instances such as beta-lactamases (*OXA-34*, *OXA-145*, *OXA-198*), aminoglycoside antibiotics
356 (*aadA3*, *aadA5*, *aadA7*), tetracyclines (*tap*, *tet(36)*, *tet(43)*), sulfonamides (*sul2*, *sul4*),
357 fluoroquinolones (*adeF*, *emrA*, *smeE*), macrolides (*macB*), rifamycins (*rpoB2*, *rphA*), and
358 glycopeptides (*vanS*) being particularly pronounced. Additionally, an examination of the relative
359 abundance of genes associated with ROS stress response (*soxR*, *oxyR*, *sodAB*, *katG*, and *ahpCF*)
360 across both DO2 and DO8 conditions revealed a consistent upregulation under the higher DO8

361 condition (Figure 3c). This pattern suggests an intensified oxidative stress response, with the
362 trend uniformly observed across all analyzed genes, indicating a systemic adaptation to the
363 elevated ROS levels correlated with higher DO concentrations. These findings helped
364 particularly in understanding the mechanisms driving ARG dynamics in CAS processes. The
365 elevated ROS levels under high DO conditions, coupled with the upregulation of oxidative stress
366 response genes, provide compelling evidence supporting our hypothesis that increased ROS, a
367 byproduct of intensive aeration in CAS systems, could be a contributing factor to the emergence
368 and persistence of ARGs.

369 **Identification of host ARBs harboring the enriched/emerged ARGs**

370 In addition to the enriched or emerged ARGs, identifying the host pathogens harboring the
371 ARGs in the CAS processes is crucial, as these ARBs determine the potential health risks.
372 Widely adopted correlation-based approaches investigate the relationships between ARGs and
373 their potential hosts in WWTPs [72], based on the rationale that host ARBs should exhibit similar
374 abundance trends as the ARGs they carry. Our comprehensive analysis using the SparCC
375 correlation approach unraveled the intricate ARG-ARB co-associations in the CAS stage of both
376 $WWTP_{Gö}$, and $WWTP_{Gw}$. The co-association networks comprised 128 nodes (41 ARBs and 87
377 ARGs) in $WWTP_{Gö}$ and 87 nodes (34 ARBs and 53 ARGs) in $WWTP_{Gw}$ (Figure 4, Figure S6,
378 Supplemental Data 4). Notable key hub ARBs in $WWTP_{Gö}$ included *Klebsiella quasipneumoniae*
379 (associated with 22 ARGs), *Pseudomonas aeruginosa* (17 ARGs), *Burkholderia pseudomallei*
380 (13 ARGs), *Phocaeicola vulgatus* (8 ARGs), *Streptococcus suis* (8 ARGs), and *Enterococcus*
381 *faecalis* (7 ARGs). In $WWTP_{Gw}$, the key hub ARBs were *Klebsiella pneumoniae* (13 ARGs),
382 *Achromobacter ruhlandii* (9 ARGs), *Delftia acidovorans* (8 ARGs), *Aeromonas salmonicida* (7
383 ARGs), *Pseudomonas aeruginosa* (7 ARGs), and *Escherichia coli* (6 ARGs). Notably, multiple

host ARBs harbored many of the same ARGs in both CAS processes. For instance, the *rpoB2* gene (conferring rifamycin resistance) was associated with 9 ARBs. Genes resistant to various drug classes, including efflux pump resistant genes (*MexD*, *mexY*, *mexQ*, *novA*, *arlS*, *mtrA*, *rsmA*, *muxC*), OXA beta-lactamase genes (*OXA-3*, *OXA-45*, *OXA-101*, *OXA-427*), and tetracycline genes (*tet(60)*, *tet(35)*), were shared among ARBs (Supplemental Data 4).

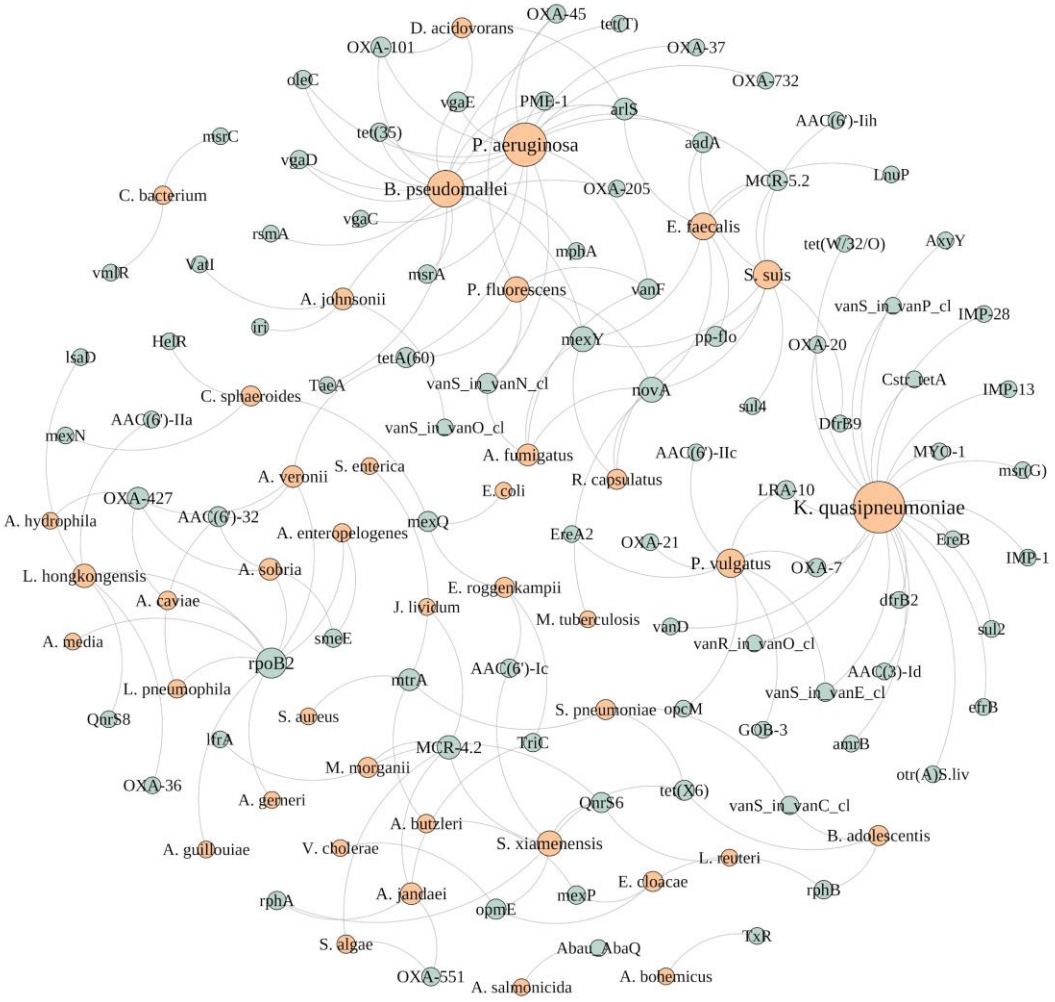

Figure 4. Network analysis depicting the co-associations between ARGs and ARBs in the CAS process in $WWTP_{Gö}$. Nodes represent individual ARGs and ARBs, with edges indicating SparCC correlations.

This sharing of ARGs suggests a specific co-selection mechanism, where host ARBs acquire and maintain ARGs, reflecting their adaptive strategies in the CAS environment. These shared ARGs

394 indicate possible HGT process in the CAS, significantly contributing to the ARG enrichment.
395 Transfer of ARGs between bacteria through HGT is a major challenge in combating AR as it
396 accelerates the rise of resistant species. Alarmingly, several ARBs belonged to the ESKAPE
397 family of clinically concerning pathogens in both $WWTP_{Gö}$ (*Staphylococcus aureus*,
398 *Pseudomonas aeruginosa*, *Enterobacter roggenkampii*, *Enterobacter cloacae*) and $WWTP_{Gw}$
399 (*Staphylococcus aureus*, *Klebsiella pneumoniae*, *Acinetobacter baumannii*, *Pseudomonas*
400 *aeruginosa*, *Enterobacter cloacae*). These ESKAPE pathogens are known to acquire antibiotic
401 resistance through HGT and have evolved a significant ability to thrive under high ROS stress
402 conditions [73], potentially contributing to ARG enrichment/emergence in the CAS processes.
403 These findings have profound public health implications, as CAS processes may inadvertently
404 promote the proliferation and dissemination of the host ARBs to the secondary clarify and finally
405 into the environment. While previous reports proposed inactivating ARGs in WWTP disinfection
406 systems [74,75], controlling the enrichment or emergence of ARBs within the CAS system should
407 be considered an alternative strategy to limit the enrichment/emergence and dissemination of
408 ARGs.

409 **Mechanism of ROS-induced ARG enrichment/emergence in CAS**

410 Sublethal concentrations of endogenous ROS can trigger a series of direct or indirect cellular
411 responses that may contribute to the enrichment/emergence of ARGs in the CAS process. These
412 responses include the activation of transcriptional regulators, expression of oxidative defense
413 enzymes, metabolic adaptations, DNA damage, activation of efflux pumps, cell damage, and
414 increased permeability and transformation potential (Figure 5a). Firstly, enhanced expression of
415 transcription factors like *oxyR* and *soxRS* facilitate the production of ROS-scavenging enzymes
416 such as superoxide dismutase, catalase, thioredoxins and others [76]. In both the $WWTP_{Gö}$ and

417 $WWTP_{Gw}$ CAS processes, we observed a high abundance of these transcription factors and ROS
418 scavengers (Figure 2b and Figure S2b). Secondly, ROS stress can disrupt the TCA cycle, leading
419 to hyperactivation of respiration, as seen in certain antibiotic treatments [77]. Previous reports also
420 suggested the disruption of the nucleotide pool, leading to the increase of ATP demand elevating
421 TCA cycle activity and cellular respiration under quinolones treatments [78]. This disruption may
422 trigger metabolic adaptations, such as activating the glyoxylate shunt (GS) [79] to reduce oxidative
423 burden or redirecting flux to the PPP for increased NADPH production, supporting antioxidant
424 defense systems [80]. Our comparative analysis revealed an enrichment of genes involved in these
425 metabolic pathways, ATP and NADPH production, and consumption in the CAS system
426 compared to other treatment processes (Figure 5b, Figure S7). Moreover, sublethal ROS levels
427 can cause DNA damage and potential mutations, facilitating the emergence of *de novo* antibiotic
428 resistance [36]. Notably, DNA repair-related genes were abundant in the CAS processes at both
429 WWTPs. We also identified several ARGs in the CAS process that were not detected in the
430 upstream processes of both WWTPs (Supplemental Data 2b). This indicates that ROS-induced
431 mutations could be responsible for their emergence. As a secondary defense, bacteria activate
432 multidrug efflux pumps to expel antibiotics from the cell, promoting antibiotic tolerance. The
433 abundance of multidrug efflux pump genes was high in the CAS processes (Figure 5b, Figure
434 S7). Additionally, oxidative damage can weaken the bacterial cell envelope, potentially leading
435 to the release of ARGs into the environment. This process, coupled with enhanced
436 transformation capabilities under oxidative stress, increases the uptake of foreign DNA,
437 including ARGs, through HGT. Increased cell permeability can promote the uptake of foreign
438 ARGs and eDNA through transformation [81]. Previous reports suggested that *Streptococcus* sp.
439 released eDNA under H_2O_2 stress [82]. A recent report revealed that phenolic compounds can

promote ROS-induced increased cell permeability and HGT [42]. These simultaneous events occurring in the CAS process under oxidative stress conditions may play a significant role in enriching ARGs or helping ARG emergence. Overall, the proposed mechanisms by which ROS can contribute to ARG enrichment/emergence in the CAS process include activation of oxidative stress responses and metabolic adaptations, DNA damage and *de novo* resistance development, increased efflux pump activity, and enhanced cell permeability promoting horizontal gene transfer facilitated by oxidative damage. This multifactorial process underscores the complex interplay between oxidative stress and antibiotic resistance in the CAS process.

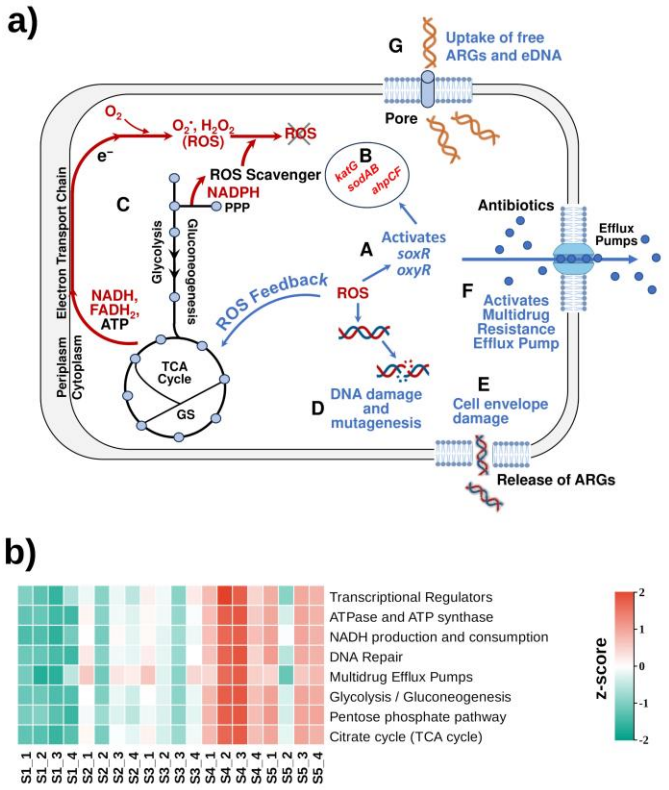

Figure 5. Mechanisms of ROS-induced ARG enrichment/emergence in the CAS process. a) A schematic illustration of the proposed mechanisms by which ROS may contribute to ARG proliferation in the CAS process. The diagram depicts the cascade of cellular responses triggered by ROS, including (A) activation of transcription factors that (B) induced expression of ROS-scavenging enzymes, (C) metabolic adaptations to mitigate ROS damage, (D) DNA damage leading to mutations, (E) cell envelope damage and ARG release, (F) activation of multidrug resistance efflux pumps, (G) uptake of free ARGs and eDNA. These responses collectively facilitate an environment

455 conducive to the proliferation and spread of ARGs in the CAS system. b) Heatmap illustrating the change in gene
456 abundances associated with the cellular processes across various stages of the $WWTP_{Gö}$.

457 **Implications**

458 Our findings shed light on the role of ROS in promoting ARG enrichment and emergence within
459 the CAS microbiome. Confirming our hypothesis, the study emphasizes the need for oxygen
460 control in WWTPs to prevent ROS-induced ARG proliferation. Additionally, we observed
461 significant differences in the ARG composition between hospital effluents or influents and the
462 WWTP effluents. Notably, the ARG profiles of WWTP effluents are more influenced by the
463 CAS resistome than the incoming wastewater composition. The majority of highly abundant
464 ARGs detected in WWTP effluents originate (enrich or emerge) from the CAS process,
465 indicating that the treatment processes, particularly within CAS systems, play a crucial role in
466 determining the resistome of discharged effluents. Thus, there is a critical need to closely
467 examine the ARG proliferation within CAS systems to reduce the ARG load in effluent
468 discharges. Also, we suggest that ARB-specific targeted approach should be adopted to control
469 the abundance of the key host pathogens harboring the ARGs in the CAS processes. Our findings
470 suggest that aeration strategies are required for lowering ARG proliferation without
471 compromising carbon and nutrient treatment efficiency.

472 **ASSOCIATED CONTENT**

473 **Supporting Information**

474 All the supplementary methods, tables and figures are provided in Supporting Information.pdf.
475 Additionally, detailed information on differentially abundant ARGs, ARG family and drug
476 classes, ARG correlation with ROS genes, and ARG-ARB co-association networks are provided
477 in Supporting Data.xlsx.

AUTHOR INFORMATION

Corresponding Author

Naresh Singhal* Phone: +64 9 923 4512; e-mail: n.singhal@auckland.ac.nz

ORCID

Bharat Manna: 0000-0001-7394-8204

Naresh Singhal: 0000-0002-9461-688X

Author Contributions

BM: Conceptualization, Experiments and metagenomics data analysis, Writing - original draft. XZ: Experiments and data analysis, Writing - review & editing. NS: Conceptualization, Funding acquisition, Supervision, Writing - review & editing.

Funding Sources

The study was funded by Marsden Award from the Royal Society of New Zealand (Contract Number: MFP-UOA2018) made to NS.

Notes

The authors declare no competing financial interest.

ACKNOWLEDGMENT

The authors acknowledge the use of New Zealand eScience Infrastructure (NeSI) high performance computing facilities, consulting support and/or training services as part of this research. New Zealand's national facilities are provided by NeSI and funded jointly by NeSI's collaborator institutions and through the Ministry of Business, Innovation & Employment's Research Infrastructure programme. URL https://www.nesi.org.nz. The authors also acknowledge the Centre for eResearch at the University of Auckland for their help in facilitating this research. http://www.eresearch.auckland.ac.nz. We thank the authors of references 45 and 46 for their generous contribution of making the metagenomic data publicly accessible, which has proven to be invaluable for this study.

504 **REFERENCES**

505 1. Murray, C. J. *et al.* Global burden of bacterial antimicrobial resistance in 2019: a
506 systematic analysis. *Lancet* (2022) doi:10.1016/S0140-6736(21)02724-0.

507 2. Centers, U. S., Control, D., Fattouh, M., El-Din, A. N. & Davies, J. Centers for Disease
508 Control and Prevention. Antibiotic resistance threats in the United States, 2019. *Int. J.*
509 *Curr. Microbiol. Appl. Sci.* (2019).

510 3. Nelson, R. E. *et al.* National estimates of healthcare costs associated with multidrug-
511 resistant bacterial infections among hospitalized patients in the United States. *Clin. Infect.*
512 *Dis.* (2021) doi:10.1093/cid/ciaa1581.

513 4. McEwen, S. A. & Collignon, P. J. Antimicrobial Resistance: a One Health Perspective.
514 *Microbiol. Spectr.* (2018) doi:10.1128/microbiolspec.arba-0009-2017.

515 5. Agga, G. E., Arthur, T. M., Durso, L. M., Harhay, D. M. & Schmidt, J. W. Antimicrobial-
516 resistant bacterial populations and antimicrobial resistance genes obtained from
517 environments impacted by livestock and municipal waste. *PLoS One* (2015)
518 doi:10.1371/journal.pone.0132586.

519 6. Rowe, W. P. M. *et al.* Overexpression of antibiotic resistance genes in hospital effluents
520 over time. *J. Antimicrob. Chemother.* (2017) doi:10.1093/jac/dkx017.

521 7. Foyle, L. *et al.* Prevalence and distribution of antimicrobial resistance in effluent
522 wastewater from animal slaughter facilities: A systematic review. *Environmental*
523 *Pollution* at https://doi.org/10.1016/j.envpol.2022.120848 (2023).

524 8. Munk, P. *et al.* Genomic analysis of sewage from 101 countries reveals global landscape
525 of antimicrobial resistance. *Nat. Commun.* (2022) doi:10.1038/s41467-022-34312-7.

526 9. Alexander, J., Hembach, N. & Schwartz, T. Evaluation of antibiotic resistance
527 dissemination by wastewater treatment plant effluents with different catchment areas in
528 Germany. *Sci. Rep.* (2020) doi:10.1038/s41598-020-65635-4.

529 10. Manaia, C. M. *et al.* Antibiotic resistance in wastewater treatment plants: Tackling the
530 black box. *Environment International* at https://doi.org/10.1016/j.envint.2018.03.044
531 (2018).

532 11. Pazda, M., Kumirska, J., Stepnowski, P. & Mulkiewicz, E. Antibiotic resistance genes
533 identified in wastewater treatment plant systems – A review. *Science of the Total*
534 *Environment* at https://doi.org/10.1016/j.scitotenv.2019.134023 (2019).

535 12. Wang, Y., Han, Y., Li, L., Liu, J. & Yan, X. Distribution, sources, and potential risks of
536 antibiotic resistance genes in wastewater treatment plant: A review. *Environmental*
537 *Pollution* at https://doi.org/10.1016/j.envpol.2022.119870 (2022).

538 13. Chen, Y. *et al.* Occurrence and fate of antibiotics, antimicrobial resistance determinants

539 and potential human pathogens in a wastewater treatment plant and their effects on
540 receiving waters in Nanjing, China. *Ecotoxicol. Environ. Saf.* (2020)
541 doi:10.1016/j.ecoenv.2020.111371.

542 14. Uluseker, C. *et al.* A Review on Occurrence and Spread of Antibiotic Resistance in
543 Wastewaters and in Wastewater Treatment Plants: Mechanisms and Perspectives.
544 *Frontiers in Microbiology* at https://doi.org/10.3389/fmicb.2021.717809 (2021).

545 15. Karkman, A., Do, T. T., Walsh, F. & Virta, M. P. J. Antibiotic-Resistance Genes in Waste
546 Water. *Trends in Microbiology* at https://doi.org/10.1016/j.tim.2017.09.005 (2018).

547 16. Wei, Z. *et al.* High-Throughput Single-Cell Technology Reveals the Contribution of
548 Horizontal Gene Transfer to Typical Antibiotic Resistance Gene Dissemination in
549 Wastewater Treatment Plants. *Environ. Sci. Technol.* (2021) doi:10.1021/acs.est.1c01250.

550 17. Korzeniewska, E., Korzeniewska, A. & Harnisz, M. Antibiotic resistant Escherichia coli
551 in hospital and municipal sewage and their emission to the environment. *Ecotoxicol.*
552 *Environ. Saf.* (2013) doi:10.1016/j.ecoenv.2013.01.014.

553 18. Hocquet, D., Muller, A. & Bertrand, X. What happens in hospitals does not stay in
554 hospitals: antibiotic-resistant bacteria in hospital wastewater systems. *Journal of Hospital*
555 *Infection* at https://doi.org/10.1016/j.jhin.2016.01.010 (2016).

556 19. Paulus, G. K. *et al.* The impact of on-site hospital wastewater treatment on the
557 downstream communal wastewater system in terms of antibiotics and antibiotic resistance
558 genes. *Int. J. Hyg. Environ. Health* (2019) doi:10.1016/j.ijheh.2019.01.004.

559 20. Mehanni, M. M. *et al.* Antibiotic-resistant bacteria in hospital wastewater treatment plant
560 effluent and the possible consequences of its reuse in agricultural irrigation. *Front.*
561 *Microbiol.* (2023) doi:10.3389/fmicb.2023.1141383.

562 21. Honda, R. *et al.* Transition of antimicrobial resistome in wastewater treatment plants:
563 impact of process configuration, geographical location and season. *npj Clean Water*
564 (2023) doi:10.1038/s41545-023-00261-x.

565 22. Luo, L. *et al.* Comparison of bacterial communities and antibiotic resistance genes in
566 oxidation ditches and membrane bioreactors. *Sci. Rep.* (2021) doi:10.1038/s41598-021-
567 88335-z.

568 23. Majeed, H. J. *et al.* Evaluation of Metagenomic-Enabled Antibiotic Resistance
569 Surveillance at a Conventional Wastewater Treatment Plant. *Front. Microbiol.* (2021)
570 doi:10.3389/fmicb.2021.657954.

571 24. Ju, F. *et al.* Wastewater treatment plant resistomes are shaped by bacterial composition,
572 genetic exchange, and upregulated expression in the effluent microbiomes. *ISME J.* (2019)
573 doi:10.1038/s41396-018-0277-8.

574 25. Liu, Z. *et al.* Metagenomic and metatranscriptomic analyses reveal activity and hosts of

575 antibiotic resistance genes in activated sludge. *Environ. Int.* (2019)
576 doi:10.1016/j.envint.2019.05.036.

577 26. Bengtsson-Palme, J. *et al.* Elucidating selection processes for antibiotic resistance in
578 sewage treatment plants using metagenomics. *Sci. Total Environ.* (2016)
579 doi:10.1016/j.scitotenv.2016.06.228.

580 27. Petrovich, M. L. *et al.* Microbial and Viral Communities and Their Antibiotic Resistance
581 Genes Throughout a Hospital Wastewater Treatment System. *Front. Microbiol.* (2020)
582 doi:10.3389/fmicb.2020.00153.

583 28. Dcosta, V. M. *et al.* Antibiotic resistance is ancient. *Nature* at
584 https://doi.org/10.1038/nature10388 (2011).

585 29. Dwyer, D. J., Kohanski, M. A. & Collins, J. J. Role of reactive oxygen species in
586 antibiotic action and resistance. *Current Opinion in Microbiology* at
587 https://doi.org/10.1016/j.mib.2009.06.018 (2009).

588 30. Van Acker, H. & Coenye, T. The Role of Reactive Oxygen Species in Antibiotic-
589 Mediated Killing of Bacteria. *Trends in Microbiology* at
590 https://doi.org/10.1016/j.tim.2016.12.008 (2017).

591 31. Lam, P. L. *et al.* The role of reactive oxygen species in the biological activity of
592 antimicrobial agents: An updated mini review. *Chemico-Biological Interactions* at
593 https://doi.org/10.1016/j.cbi.2020.109023 (2020).

594 32. Imlay, J. A. Pathways of Oxidative Damage. *Annual Review of Microbiology* at
595 https://doi.org/10.1146/annurev.micro.57.030502.090938 (2003).

596 33. Imlay, J. A. Where in the world do bacteria experience oxidative stress? *Environmental*
597 *Microbiology* at https://doi.org/10.1111/1462-2920.14445 (2019).

598 34. Li, H. *et al.* Reactive Oxygen Species in Pathogen Clearance: The Killing Mechanisms,
599 the Adaption Response, and the Side Effects. *Frontiers in Microbiology* at
600 https://doi.org/10.3389/fmicb.2020.622534 (2021).

601 35. Fang, F. C. Antimicrobial actions of reactive oxygen species. *MBio* (2011)
602 doi:10.1128/mBio.00141-11.

603 36. Qi, W., Jonker, M. J., Teichmann, L., Wortel, M. & ter Kuile, B. H. The influence of
604 oxygen and oxidative stress on de novo acquisition of antibiotic resistance in E. coli and
605 Lactobacillus lactis. *BMC Microbiol.* **23**, 1–14 (2023).

606 37. Ariza, R. R., Cohen, S. P., Bachhawat, N., Levy, S. B. & Demple, B. Repressor mutations
607 in the marRAB operon that activate oxidative stress genes and multiple antibiotic
608 resistance in Escherichia coli. *J. Bacteriol.* (1994) doi:10.1128/jb.176.1.143-148.1994.

609 38. Mandsberg, L. F. *et al.* Antibiotic resistance in Pseudomonas aeruginosa strains with

610 increased mutation frequency due to inactivation of the DNA oxidative repair system.
611 *Antimicrob. Agents Chemother.* (2009) doi:10.1128/AAC.00428-08.

612 39. Jin, M. *et al.* Antidepressant fluoxetine induces multiple antibiotics resistance in
613 Escherichia coli via ROS-mediated mutagenesis. *Environ. Int.* (2018)
614 doi:10.1016/j.envint.2018.07.046.

615 40. Sulfikar, Honda, R., Noguchi, M., Yamamoto-Ikemoto, R. & Watanabe, T. Effect of
616 sedimentation and aeration on antibiotic resistance induction in the activated sludge
617 process. *J. Water Environ. Technol.* (2018) doi:10.2965/jwet.17-046.

618 41. Tan, Q. *et al.* Triclosan weakens the nitrification process of activated sludge and increases
619 the risk of the spread of antibiotic resistance genes. *J. Hazard. Mater.* (2021)
620 doi:10.1016/j.jhazmat.2021.126085.

621 42. Ma, X. *et al.* Phenolic compounds promote the horizontal transfer of antibiotic resistance
622 genes in activated sludge. *Sci. Total Environ.* (2021) doi:10.1016/j.scitotenv.2021.149549.

623 43. Hendriksen, R. S. *et al.* Global monitoring of antimicrobial resistance based on
624 metagenomics analyses of urban sewage. *Nat. Commun.* (2019) doi:10.1038/s41467-019-
625 08853-3.

626 44. Lira, F., Vaz-Moreira, I., Tamames, J., Manaia, C. M. & Martínez, J. L. Metagenomic
627 analysis of an urban resistome before and after wastewater treatment. *Sci. Rep.* (2020)
628 doi:10.1038/s41598-020-65031-y.

629 45. Schneider, D., Aßmann, N., Wicke, D., Poehlein, A. & Daniel, R. Metagenomes of
630 Wastewater at Different Treatment Stages in Central Germany. *Microbiol. Resour.*
631 *Announc.* (2020) doi:10.1128/mra.00201-20.

632 46. Schneider, D., Zühlke, D., Poehlein, A., Riedel, K. & Daniel, R. Metagenome-Assembled
633 Genome Sequences from Different Wastewater Treatment Stages in Germany. *Microbiol.*
634 *Resour. Announc.* (2021) doi:10.1128/mra.00504-21.

635 47. Bolger, A. M., Lohse, M. & Usadel, B. Trimmomatic: A flexible trimmer for Illumina
636 sequence data. *Bioinformatics* (2014) doi:10.1093/bioinformatics/btu170.

637 48. Raes, E. J. *et al.* Metabolic pathways inferred from a bacterial marker gene illuminate
638 ecological changes across South Pacific frontal boundaries. *Nat. Commun.* (2021)
639 doi:10.1038/s41467-021-22409-4.

640 49. Tamames, J. & Puente-Sánchez, F. SqueezeMeta, a highly portable, fully automatic
641 metagenomic analysis pipeline. *Front. Microbiol.* (2019) doi:10.3389/fmicb.2018.03349.

642 50. Li, D., Liu, C. M., Luo, R., Sadakane, K. & Lam, T. W. MEGAHIT: An ultra-fast single-
643 node solution for large and complex metagenomics assembly via succinct de Bruijn graph.
644 *Bioinformatics* (2015) doi:10.1093/bioinformatics/btv033.

645 51. Schmieder, R. & Edwards, R. Quality control and preprocessing of metagenomic datasets.
646 *Bioinformatics* (2011) doi:10.1093/bioinformatics/btr026.

647 52. Seemann, T. Prokka: Rapid prokaryotic genome annotation. *Bioinformatics* (2014)
648 doi:10.1093/bioinformatics/btu153.

649 53. Hyatt, D. *et al.* Prodigal: Prokaryotic gene recognition and translation initiation site
650 identification. *BMC Bioinformatics* (2010) doi:10.1186/1471-2105-11-119.

651 54. Clark, K., Karsch-Mizrachi, I., Lipman, D. J., Ostell, J. & Sayers, E. W. GenBank.
652 *Nucleic Acids Res.* (2016) doi:10.1093/nar/gkv1276.

653 55. Kanehisa, M. & Goto, S. KEGG: Kyoto Encyclopedia of Genes and Genomes. *Nucleic*
654 *Acids Research* at https://doi.org/10.1093/nar/28.1.27 (2000).

655 56. Buchfink, B., Xie, C. & Huson, D. H. Fast and sensitive protein alignment using
656 DIAMOND. *Nature Methods* at https://doi.org/10.1038/nmeth.3176 (2014).

657 57. Alcock, B. P. *et al.* CARD 2020: Antibiotic resistome surveillance with the
658 comprehensive antibiotic resistance database. *Nucleic Acids Res.* (2020)
659 doi:10.1093/nar/gkz935.

660 58. Langmead, B. & Salzberg, S. L. Fast gapped-read alignment with Bowtie 2. *Nat. Methods*
661 (2012) doi:10.1038/nmeth.1923.

662 59. Puente-Sánchez, F., Garciá-Garciá, N. & Tamames, J. SQMtools: Automated processing
663 and visual analysis of 'omics data with R and anvi'o. *BMC Bioinformatics* (2020)
664 doi:10.1186/s12859-020-03703-2.

665 60. Paulson, J. N., Colin Stine, O., Bravo, H. C. & Pop, M. Differential abundance analysis
666 for microbial marker-gene surveys. *Nat. Methods* (2013) doi:10.1038/nmeth.2658.

667 61. Dhariwal, A. *et al.* MicrobiomeAnalyst: A web-based tool for comprehensive statistical,
668 visual and meta-analysis of microbiome data. *Nucleic Acids Res.* (2017)
669 doi:10.1093/nar/gkx295.

670 62. Chen, C. *et al.* TBtools: An Integrative Toolkit Developed for Interactive Analyses of Big
671 Biological Data. *Mol. Plant* (2020) doi:10.1016/j.molp.2020.06.009.

672 63. Robinson Mark, D., McCarthy Davis, J. & Smyth Gordon, K. edgeR: a Bioconductor
673 package for differential expression analysis of digital gene expression data. *Bioinformatics*
674 (2010).

675 64. Friedman, J. & Alm, E. J. Inferring Correlation Networks from Genomic Survey Data.
676 *PLoS Comput. Biol.* (2012) doi:10.1371/journal.pcbi.1002687.

677 65. Bastian, M., Heymann, S. & Jacomy, M. Gephi: An Open Source Software for Exploring
678 and Manipulating Networks. in *Proceedings of the 3rd International AAAI Conference on*

679 *Weblogs and Social Media, ICWSM 2009* (2009). doi:10.1609/icwsm.v3i1.13937.

680 66. Wickham, H. ggplot2. *Wiley Interdiscip. Rev. Comput. Stat.* (2011) doi:10.1002/wics.147.

681 67. R Core Team. R Core Team 2021 R: A language and environment for statistical
682 computing. R foundation for statistical computing. https://www.R-project.org/. *R Found.*
683 *Stat. Comput.* (2022).

684 68. Seo, S. W., Kim, D., Szubin, R. & Palsson, B. O. Genome-wide Reconstruction of OxyR
685 and SoxRS Transcriptional Regulatory Networks under Oxidative Stress in Escherichia
686 coli K-12 MG1655. *Cell Rep.* (2015) doi:10.1016/j.celrep.2015.07.043.

687 69. Wei, Q. *et al.* Global regulation of gene expression by OxyR in an important human
688 opportunistic pathogen. *Nucleic Acids Res.* (2012) doi:10.1093/nar/gks017.

689 70. Lau, G. W., Britigan, B. E. & Hassett, D. J. Pseudomonas aeruginosa OxyR is required for
690 full virulence in rodent and insect models of infection and for resistance to human
691 neutrophils. *Infect. Immun.* (2005) doi:10.1128/IAI.73.4.2550-2553.2005.

692 71. Wang, P. *et al.* SoxS is a positive regulator of key pathogenesis genes and promotes
693 intracellular replication and virulence of Salmonella Typhimurium. *Microb. Pathog.*
694 (2020) doi:10.1016/j.micpath.2019.103925.

695 72. Ju, F. *et al.* Antibiotic resistance genes and human bacterial pathogens: Co-occurrence,
696 removal, and enrichment in municipal sewage sludge digesters. *Water Res.* (2016)
697 doi:10.1016/j.watres.2015.11.071.

698 73. da Cruz Nizer, W. S. *et al.* Oxidative stress response in pseudomonas aeruginosa.
699 *Pathogens* at https://doi.org/10.3390/pathogens10091187 (2021).

700 74. Dodd, M. C. Potential impacts of disinfection processes on elimination and deactivation of
701 antibiotic resistance genes during water and wastewater treatment. *Journal of*
702 *Environmental Monitoring* at https://doi.org/10.1039/c2em00006g (2012).

703 75. Pruden, A. *et al.* Management options for reducing the release of antibiotics and antibiotic
704 resistance genes to the environment. *Environmental Health Perspectives* at
705 https://doi.org/10.1289/ehp.1206446 (2013).

706 76. Imlay, J. A. Cellular defenses against superoxide and hydrogen peroxide. *Annual Review*
707 *of Biochemistry* at https://doi.org/10.1146/annurev.biochem.77.061606.161055 (2008).

708 77. Kohanski, M. A., Dwyer, D. J., Wierzbowski, J., Cottarel, G. & Collins, J. J.
709 Mistranslation of Membrane Proteins and Two-Component System Activation Trigger
710 Antibiotic-Mediated Cell Death. *Cell* (2008) doi:10.1016/j.cell.2008.09.038.

711 78. Yang, J. H. *et al.* A White-Box Machine Learning Approach for Revealing Antibiotic
712 Mechanisms of Action. *Cell* (2019) doi:10.1016/j.cell.2019.04.016.

713 79. Lemire, J., Alhasawi, A., Appanna, V. P., Tharmalingam, S. & Appanna, V. D. Metabolic
714 defence against oxidative stress: the road less travelled so far. *Journal of Applied*
715 *Microbiology* at https://doi.org/10.1111/jam.13509 (2017).

716 80. Christodoulou, D. *et al.* Reserve Flux Capacity in the Pentose Phosphate Pathway Enables
717 Escherichia coli's Rapid Response to Oxidative Stress. *Cell Syst.* (2018)
718 doi:10.1016/j.cels.2018.04.009.

719 81. Wang, Y. *et al.* Non-antibiotic pharmaceuticals enhance the transmission of exogenous
720 antibiotic resistance genes through bacterial transformation. *ISME J.* (2020)
721 doi:10.1038/s41396-020-0679-2.

722 82. Itzek, A., Zheng, L., Chen, Z., Merritt, J. & Kreth, J. Hydrogen peroxide-dependent DNA
723 release and transfer of antibiotic resistance genes in Streptococcus gordonii. *J. Bacteriol.*
724 (2011) doi:10.1128/JB.05791-11.

725